Fluctuation and Correlation in Crystalline Lysozyme

Stéphanie Héry,[‡] Daniel Genest,[†] and Jeremy C. Smith*[,‡]

Section de Biophysique des Protéines et des Membranes, DBCM CEA-Saclay, 91191 Gif-sur-Yvette Cedex, France, and Centre de Biophysique Moléculaire, CNRS, Rue Charles Sadron, 45071 Orléans Cedex 02, France

Received June 17, 1997[⊗]

We examine interatomic distance fluctuations and displacement correlations in orthorhombic hen egg-white lysozyme using results from a 1 ns molecular dynamics trajectory of the crystalline unit cell. It is found that locally in the sequence the atoms are both highly correlated and undergo low relative fluctuations. Those nonlocal elements of the structure that undergo low relative fluctuations are located largely within secondary structural elements in the β domain. The canonical correlation matrices of the four lysozyme molecules in the unit cell are markedly different and have not converged.

INTRODUCTION

To deepen our understanding of the functional mechanisms of proteins requires an understanding of their internal motions. Picosecond and nanosecond time scale dynamics in native proteins are of particular interest as they are accessible to molecular dynamics (MD) simulation and because at physiological temperatures they manifest an intriguing variety of vibrational and diffusive motion.

A combination of experiment and simulation is necessary to characterize fully the composition of atomic motions present in proteins. Vibrations in proteins can be conveniently examined using normal mode analysis. The results of such analyses are a variety of vibrations, with frequencies upward of a few centimeters^{-1}. The lowest frequency modes are mostly large amplitude, delocalized, correlated vibrations. Neutron scattering experiments on bovine pancreatic trypsin inhibitor (BPTI) have been combined with normal mode analysis of the isolated protein.[1] The results demonstrated that low-frequency (<50 cm^{-1}) underdamped vibrations do exist in the protein. The low-frequency portion of the vibrational density of states of BPTI has been determined experimentally.[2] Subsequently, attempts were made to reproduce this frequency distribution using MD simulation.[2−5] Improved agreement between the normal modes and experiment was obtained by introducing a friction coefficient for each mode in a damped Langevin oscillator description.[2] The distribution of friction coefficients obtained by fitting to experiment is such that the very lowest frequency modes predicted by harmonic models (<15 cm^{-1}) do not vibrate at the calculated frequencies. They are either absent or overdamped. This damping scheme is in quantitative agreement with MD results[6] and with the frictional characteristics of low-frequency vibrations coupled to electronic excitation in photosynthetic reaction centers, identified by femtosecond spectroscopic experiments.[7]

Above ~200 K there is a nonvibrational component to protein dynamics that has been detected using several experimental techniques.[8,9] The dynamical transition is also present in MD simulations.[10] There is evidence that the nonvibrational dynamics may be of importance for the functioning of some proteins, *e.g.*, in ligand binding[11] or proton transfer reactions.[12] Measurements on bacteriorhodopsin have shown that the ability of the protein to functionally relax and complete its photocycle is correlated with the onset of anharmonic dynamics in the membrane.[12]

Various models for the nonvibrational atomic motions in proteins at 300 K have been proposed. Some are based on the idea of transitions between conformational substates and assume individual or collective stochastic jump dynamics of the atoms between minima on the potential energy surface of the folded protein.[9,13] In a recent MD analysis of neutron scattering data the individual side-chains of myoglobin were considered as rigid subunits and their contribution to the neutron scattering profiles of myoglobin at physiological temperatures was calculated.[14,15] The rigid side-chain displacements were found to account almost completely for the scattering profiles and could be described as continuous diffusion.

Molecular dynamics simulation has shown that the very low-frequency vibrations of myoglobin can be described in terms of rigid-helix motions.[6] However, rigid-helix motions contribute only about 30% of the mean-square displacements of helix atoms in this protein. A simplified description of the large-amplitude internal helix motions in polyalanine and myoglobin has recently been given.[16]

Ligand binding and cooperativity often require conformational change involving correlated displacements of atoms.[19] A simple model for long-distance transmission of information across a protein involves the activation and amplification of correlated motions that are present in the unperturbed protein. Although long-range correlated displacements are required for function in some proteins, it is not clear to what extent they contribute to equilibrium thermal fluctuations in proteins. It is therefore important to know whether equilibrium motions in proteins can indeed be correlated over long distances or whether anharmonic and damping effects prevent this.

The very diffuse X-ray scattering found in crystals of lysozyme and insulin has been described in terms of "liquid-like" motions,[17,18] using a phenomenological model of random atomic displacements correlated over distances <6.0 Å. This description excludes contributions to the scattering arising from correlations over longer distances. To further

[†] Centre de Biophysique Moléculaire.
[‡] Section de Biophysique des Protéines et des Membranes.
[⊗] Abstract published in *Advance ACS Abstracts,* November 1, 1997.

S0095-2338(97)00234-5 CCC: $14.00

examine the dynamical origins of X-ray diffuse scattering by proteins experimental scattering was measured from orthorhombic lysozyme crystals and compared to patterns calculated using normal mode analysis and MD simulation.[20] Only the 15 very lowest-frequency modes from the harmonic analysis were required to produce a converged pattern. This is partly because the lowest-frequency modes dominate the mean-square displacements in the harmonic approximation and partly because they are correlated over many atoms, the diffuse scattering intensity being proportional to the number of atoms involved. The average position of the diffuse ring is reproduced by both the normal modes and the molecular dynamics. However, a closer examination suggests that the fine details are better reproduced by the normal modes.

That the X-ray scattering pattern obtained from a harmonic description of the lysozyme dynamics is in reasonable accord with the observed data is consistent with the idea that intramolecular displacements correlated over long distances can exist, in contrast to the conclusions of the previous analyses of lysozyme and insulin.[17,18] However, as discussed in ref 15 a large fraction of the atomic displacements at 300 K may indeed originate from liquid-like motions, meaning nonvibrational, diffusive dynamics.[6,15]

That nonvibrational, diffusive motions exist in proteins does not contradict the above-mentioned simulation/diffuse scattering results for lysozyme. The correlated motions visible in the X-ray pattern can be diffusive or vibrational. Frictional damping of the modes, as would be incorporated in a damped Langevin oscillator description, for example, does not affect the amplitudes and forms of the modes. Therefore, frictional damping would not affect the calculated diffuse scattering, as the diffuse scattering does not depend on the time evolution of the atomic displacements, that is, whether they vibrate or not. Thus, it is conceivable that the modes contributing to the diffuse scattering pattern are a combination of under-damped and over-damped vibrations, the latter containing a diffusive element.

Work clearly needs to be pursued on examining fluctuations and correlations in protein motions in a way that permits rigorous comparison with experiment and attribution of experimentally-observed quantities. The present paper works toward this aim, by examining atomic motions and their collective and/or correlated character in a nanosecond MD trajectory of crystalline hen egg-white lysozyme. While difficult to obtain experimentally, information on correlations and fluctuations can be extracted from MD simulation.

METHODS

The Simulation. The present work involves a MD simulation of hen egg-white lysozyme—a small enzyme of 129 residues in one polypeptide chain, with a molecular weight of 14 600 Daltons. This protein consists of two domains, α and β, shown in Figure 1. About 40% of the residues belong to helices. Four disulfide bridges stabilize the structure. The active site is in the cleft between the two domains.

The starting structure for the MD simulation was obtained by X-ray diffraction at 2 Å resolution[21] and includes 111 crystallographically-observed water molecules. The crystal form is orthorhombic, $P2_12_12_1$, with unit cell parameters $a = 56.4$, $b = 73.8$, and $c = 30.5$ Å. This form is stable at physiological temperatures. The protein contains 1001 heavy atoms. The hydrogen atoms were built using the HBUILD module of CHARMM. The water molecules were modeled using the TIP3P potential.[22]

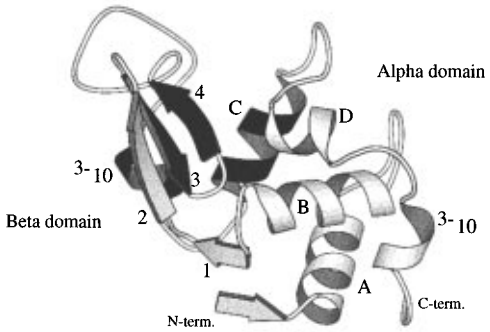

Figure 1. Lysozyme molecule. The molecule has two domains: α between residues 1−35 and 85−129 and β between residues 36−84. A region for which the fluctuations $F_{ij} < 0.5$ Å is in black. This region can be considered as a rigid group.

The MD simulation used for the present analysis was of a complete unit cell of orthorhombic lysozyme, replicated with periodic boundary conditions. The primary simulation box was the unit cell, containing four lysozyme molecules which were allowed to move in the simulation without any symmetry constraints on their relative positions. Two thousand thirty-six water molecules were also included in the simulation, including those crystallographically resolved and 32 chloride ions. The density of the system simulated is 1.243 g/mL, compared with 1.240 g/mL obtained experimentally.[23]

The MD simulation was pursued for 1 ns at 300 K in the microcanonical ensemble using the CHARMM program.[24] A cutoff distance of 9 Å was set for the computation of nonbonded interactions. The van der Waals and electrostatic terms were multiplied by a cubic switching function to smoothly reduce the potential energy to zero between 5.0 and 9.0 Å. For the MD simulation all the bonds were constrained using the SHAKE algorithm[25] to enable an integration step size of 2 fs.

In the present paper we consider only intramolecular motions in the protein. In the analysis of the correlations, the calculations were performed for each of the four molecules and averaged. All fluctuation and correlation results presented here were obtained for the backbone heavy atoms (N, C_α, C).

Fluctuations. The fluctuation matrix, F_{ij}, was calculated as follows

$$F_{ij} = \sqrt{\langle D_{ij}^2(k)\rangle - \langle D_{ij}(k)\rangle^2} \qquad (1)$$

where the averages are performed over the MD configurations, k, and the distance $D_{ij}(k)$ between two given atoms i,j is given by

$$D_{ij}(k) = \sqrt{(x_j^k - x_i^k)^2 + (y_j^k - y_i^k)^2 + (z_j^k - z_i^k)^2} \qquad (2)$$

Thus F_{ij} has a simple interpretation, being the interatomic distance fluctuation. For an arbitrarily low value of F_{ij} the atoms concerned can be considered to form part of a rigid body. For the computation of F_{ij}, the trajectories of the four lysozyme molecules were concatenated, leading to one 4 ns equivalent trajectory file for one protein molecule.

Correlations. The study of cross-correlations is a useful way of examining collective motions in proteins. Ichiye and Karplus[26] examined cross-correlations in simulations of the bovine pancreatic trypsin inhibitor using the following function

$$c(i,j) = \frac{\langle \Delta\vec{r}_i \cdot \Delta\vec{r}_j \rangle}{\langle \Delta\vec{r}_i^{\,2} \rangle^{1/2} \langle \Delta\vec{r}_j^{\,2} \rangle^{1/2}} \tag{3}$$

where $\Delta\vec{r}_i$ and $\Delta\vec{r}_j$ are the position fluctuations of atoms i and j, respectively.

$c(i, j)$ as expressed in eq 3 depends on both the correlation and the relative orientation of the fluctuations, and this leads to ambiguity in its interpretation. For example, two atoms i and j for whom $\Delta\vec{r}_i$ and $\Delta\vec{r}_j$ are orthogonal will possess a correlation coefficient that is zero even if their motions are perfectly synchronous. This is due to the fact that this method does not take into account possible correlations between different fluctuation components of a given atom or between nonhomonimic components of different atoms.

Recently a method has been proposed that avoids the above limitation.[27] This method is based on a canonical statistical analysis used for comparing different groups of variables.[28] Here we consider only correlations between pairs of atoms. For an atom i, the variables are the normalized fluctuation components, δu_i^k:

$$\delta u_i^k = \frac{(u_i^k - \langle u_i^k \rangle)}{[\langle (u_i^k - \langle u_i^k \rangle)^2 \rangle]^{1/2}} \tag{4}$$

where $u_i^k = x_i$, y_i, or z_i, for $k = 1$, 2, or 3, respectively. The angular brackets represent time averages. Identical expressions define the variables δu_j^l corresponding to atom j.

The correlation coefficient between any pair of variables related to atoms i and/or j is an element of one of the following matrices:

$$R_{ii}(k,l) = \langle \delta u_i^k \delta u_i^l \rangle$$
$$R_{jj}(k,l) = \langle \delta u_j^k \delta u_j^l \rangle$$
$$R_{ij}(k,l) = \langle \delta u_i^k \delta u_j^l \rangle$$
$$R_{ji}(k,l) = \langle \delta u_j^k \delta u_i^l \rangle$$

The problem we are interested in is to define a correlation coefficient between the two atoms i and j and not between pairs of variables. To suppress the orientation dependence, new sets of variables, $\{X_i^k, k = 1, 3\}$ and $\{X_j^l, l = 1, 3\}$ are defined. The X_i^k's and X_j^l's are called *canonical variables* and are linear combinations of the initial variables δu_i^k and δu_j^l, respectively. Thus, they span the same sub-spaces as the initial variables. They are chosen such that

$$\langle X_i^k X_i^l \rangle = \delta_{kl}$$
$$\langle X_j^k X_j^l \rangle = \delta_{kl}$$
$$\langle X_i^k X_j^l \rangle = q_k \delta_{kl}$$
$$\langle X_j^k X_i^l \rangle = q_k \delta_{kl}$$

This means that the canonical variables belonging to a same atom are uncorrelated, and a canonical variable X_i^k of group i is correlated at most with one canonical variable X_j^l of group j, q_k being the corresponding canonical coefficient.

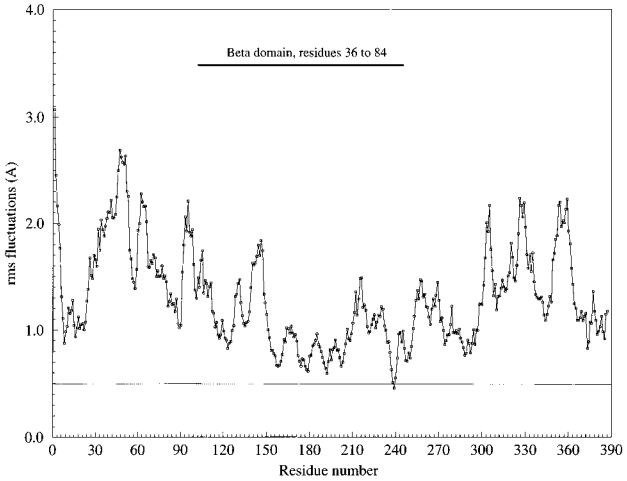

Figure 2. RMS fluctuations obtained for each N, C_α, C atom from the 4 ns concatenated trajectory.

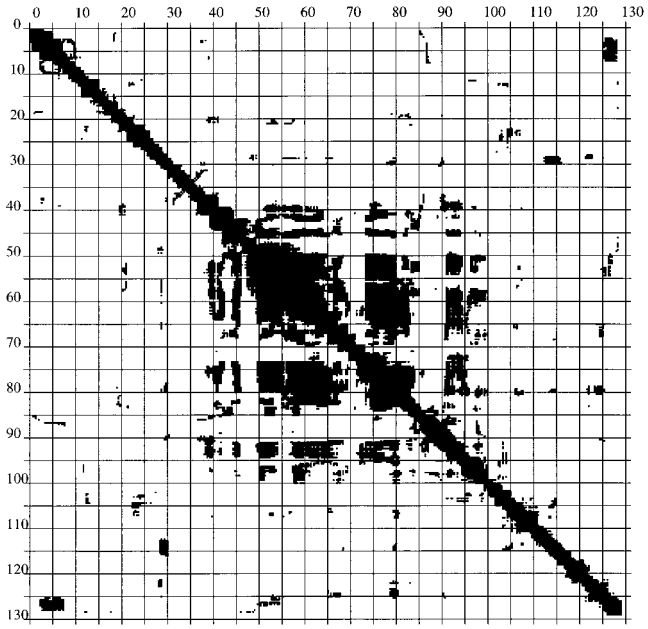

Figure 3. Fluctuation map calculated from distance fluctuation matrix, F_{ij} from the 4 ns equivalent trajectory of crystalline lysozyme. A black square indicates $F_{ij} < 0.5$ Å.

It can be shown[28] that the squares of the q_k's are the eigenvalues of the square matrix $R = R_{ii}^{-1} R_{ij} R_{jj}^{-1} R_{ji}$. Therefore, we can define a correlation coefficient C_{ij}, which expresses an average correlation between groups i and j as follows:

$$C_{ij} = \left[\frac{1}{3} Trace(R)\right]^{1/2} \tag{5}$$

The coefficient C_{ij} is defined for each pair of atoms (i, j). For perfectly correlated or anticorrelated atomic fluctuations $C_{ij} = 1$, whereas $C_{ij} = 0$ only for uncorrelated motions.

The correlation coefficient C_{ij} is calculated from correlations in fluctuations of atomic positions. For this reason the concatenation of the trajectories of the four lysozyme molecules leads to artefacts in the calculated C_{ij} (large nondynamical correlations) due to the presence of large changes in structure at the points at which the trajectories are joined. Therefore, the C_{ij} calculated here were obtained

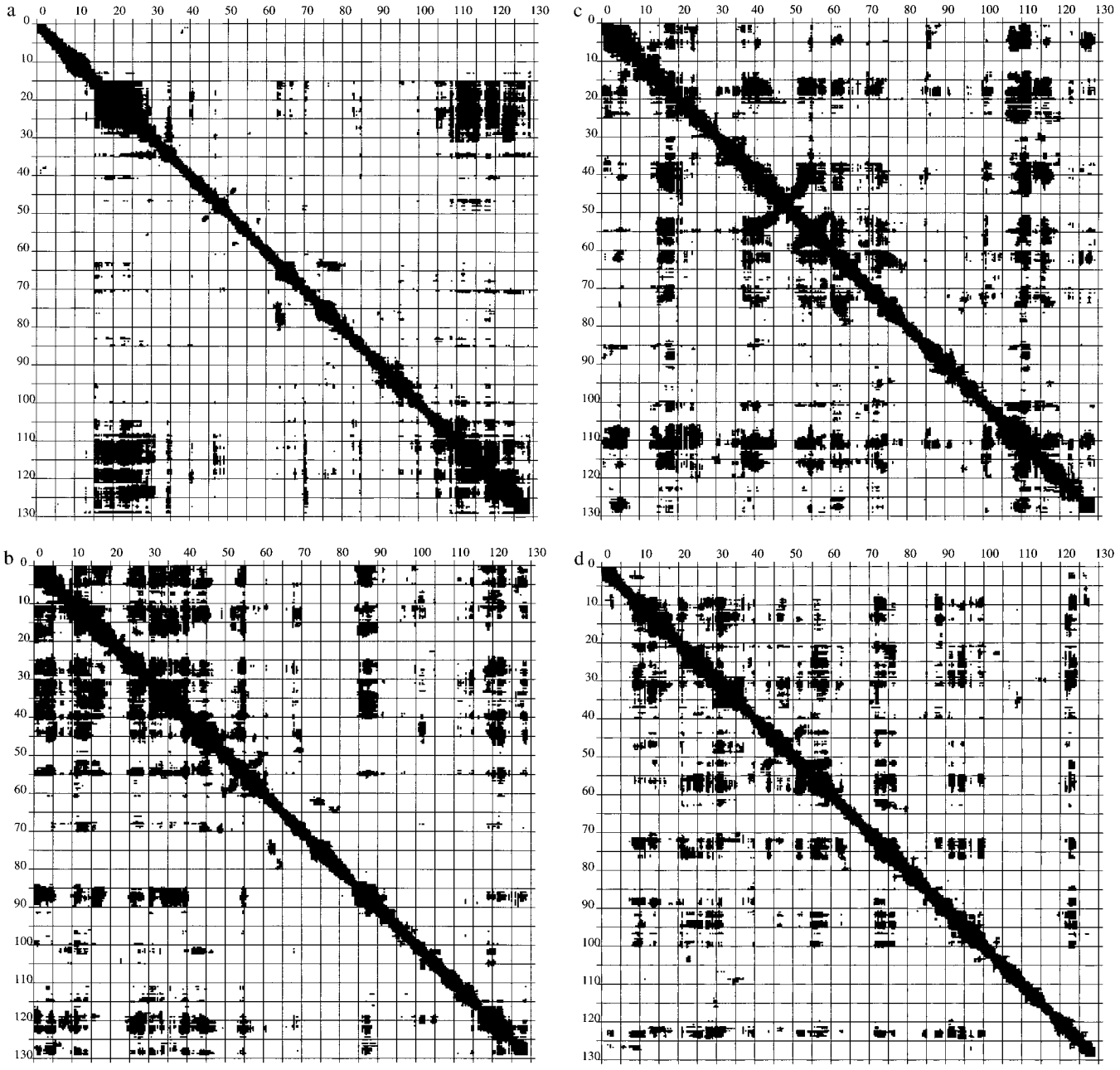

Figure 4. (a−d) Correlation maps calculated from C_{ij} matrix for each of the four molecules of crystalline lysozyme. A black square indicates $C_{ij} > 0.5$.

by averaging the C_{ij} determined for the four individual molecules.

RESULTS

In Figure 2 are presented the RMS fluctuations of the atomic positions, $\langle \Delta r_i^2 \rangle^{1/2}$, for the 4 ns of trajectory. This figure shows that the β domain residues (36−84) fluctuate less on average than those of the α domain (the average $\langle \Delta r_i^2 \rangle^{1/2}$ obtained for the α and β domains are 1.49 and 1.00 Å, respectively). In Figure 3 is presented a fluctuation map calculated from the interatomic distance fluctuation matrix, F_{ij}, given by eq 1. Most values of $\langle \Delta r_i^2 \rangle^{1/2}$ are >0.5 Å. The threshold, F_{cut} for the discrete fluctuation map representation in Figure 3 is chosen to be at $F_{cut} = 0.5$ Å, *i.e.*, a filled square at *i,j* indicates $F_{ij} < 0.5$ Å. F_{cut} is a small value of the interatomic fluctuation, as would be obtained, for example, from vibrational displacement without significant conformational change.

The black regions close to the diagonal in Figure 3 indicate that there are low relative fluctuations for atoms belonging to residues close in the sequence. This is due to the restrictions in relative motion imposed by the covalent bonding structure in the protein. Further away from the diagonal black regions correspond to low relative fluctuations between elements further away in the sequence. These are mostly situated in the region containing residues 40−100, *i.e.*; in the β domain but also including helix C (residues 89−97). Within this region several features are seen. Among these are two extended diagonal blocks; residues 47−67 (strands 3 and 4 of the β sheet plus the three associated loops) and 74−84 (the 3_{10} helix on the C-terminal end of the β domain)). A prominent off-diagonal block is also seen, indicating low relative fluctuations between the above-mentioned 47−67 and 74−84 regions. These results indicate that there is a region of the protein that acts as a relatively rigid body, consisting of three elements of secondary

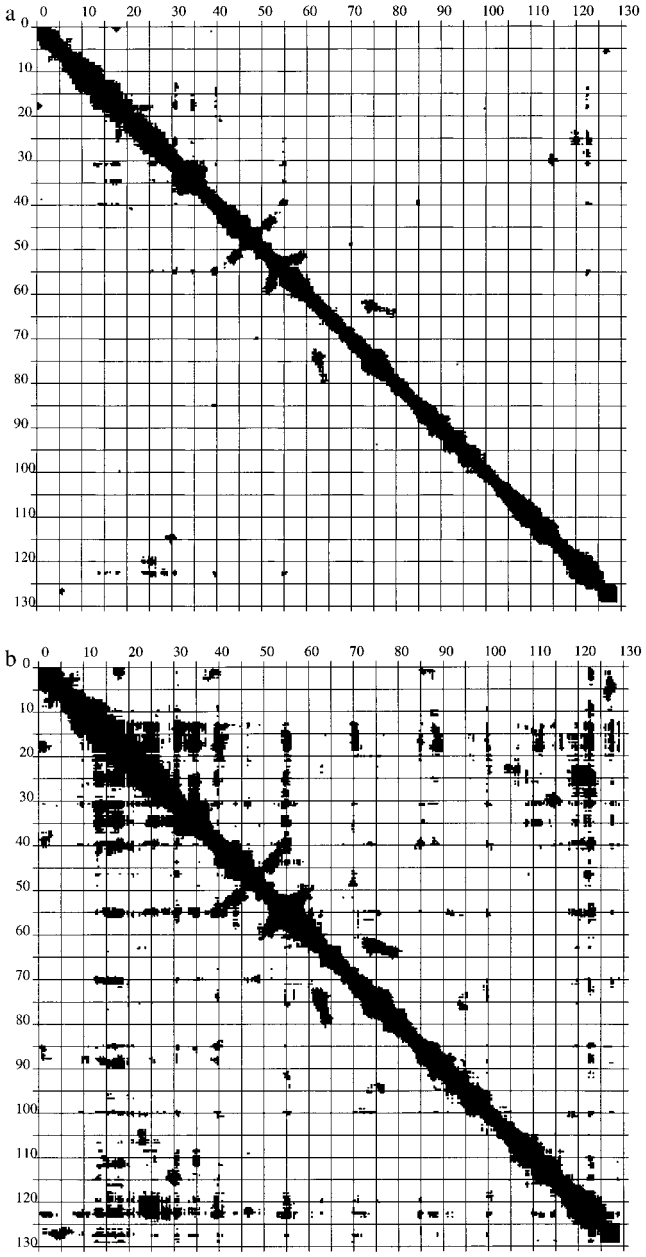

Figure 5. Correlation maps averaged over the four molecules. (a) A black square indicates $C_{ij} > 0.5$. (b) A black square indicates $C_{ij} > 0.45$.

structure in the β domain (the 3_{10} helix and two β strands) and one from the α domain (helix C). This rigid region is represented in black on Figure 1. Another small diagonal block involving residues 1−7 including the N terminal β strand and the following coil is also visible on Figure 3.

In Figure 4a−d are presented correlation maps calculated from the matrix C_{ij} obtained from the MD trajectory for each lysozyme molecule using eq 5. In a recent study on DNA[29] the degree of correlation was empirically classified as follows:

$$C_{ij} < 0.25 \quad \text{weak}$$
$$0.25 \leqslant C_{ij} < 0.50 \quad \text{moderate}$$
$$0.50 \leqslant C_{ij} < 0.75 \quad \text{strong}$$
$$0.75 \leqslant C_{ij} \leqslant 1.00 \quad \text{very strong}$$

In Figure 4 a threshold of 0.5 is selected, *i.e.*, corresponding to strong correlations. Excepting for the diagonal region,

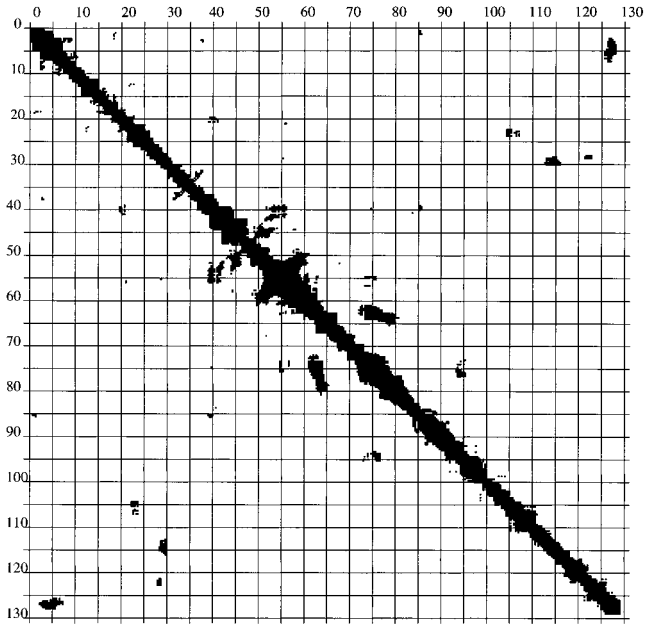

Figure 6. Regions of low relative fluctuation and high correlation. A black square corresponds to pairs of atoms for which $F_{ij} < 0.5$ Å and $C_{ij} > 0.45$.

which is present in all the maps and extends over ∼3 residues, different regions are correlated in the four molecules. In Figure 4a two major regions involve residues 15−27 (including helix A) and 105−129 (helix D, the 3_{10} helix and their connecting loops). In Figure 4b strong correlation is found between residues in the N-terminal region 1−45 (corresponding to part of the α domain and strands 1 and 2 of the β domain). In Figure 4c three sparse regions exist indicating correlation involving residues 1−20 (the first strand and helix A in the α domain), 37−75 (four strands of the β domain), and 100−120 (helix D). In Figure 4d small diagonal and off-diagonal blocks can be distinguished, involving residues 10−20 (C-terminal end of helix A), 30−37 (C-terminal end of helix B), and 50−60 (strand 3 and 4).

Figure 5a,b show correlation matrix maps obtained by averaging C_{ij} over the four molecules, with cut-offs of 0.5 and 0.45, respectively. This confirms the presence of strong local correlations for ∼3 residues along the sequence, as evidenced by the thickness of the close-to-diagonal region. Some other small regions of strong correlations (Figure 5a) involving 5 to 8 residues are visible close to the diagonal, for example residues 30−37, *i. e.*, the C-terminal part of helix B, and residues 52−60 which are strand 3 and parts of the connecting loops. With the lower cut-off, in Figure 5b, numerous regions of moderate correlation appear. The most extensive is situated between residues 12−40, containing the C-terminal end of helix A, helix B and strand 1. The 50−60 region corresponding to strands 3 and 4 also contains correlations. Also of interest are the off-diagonal correlations between residues 119−124 (C-terminal 3_{10} helix) and residues 22−28 (N-terminal part of helix B).

Perhaps the most striking result is to be found when comparing the off-diagonal regions of Figures 3 and 5. Clearly, the regions of strong correlation mostly do not match those of low interatomic fluctuation. In Figure 6 are shown the regions of both low relative fluctuation and at least moderate correlation, *i.e.*, a black square corresponds to pairs of atoms for which $F_{ij} < 0.5$ Å and $C_{ij} > 0.45$. Atoms satisfying these criteria belong to rigid bodies undergoing

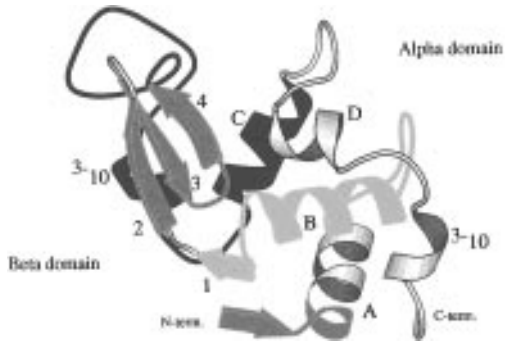

Figure 7. Representation of the lysozyme molecule with its secondary structural elements. Dark blue: regions where $F_{ij} < 0.5$ Å from Figure 3. Orange: diagonal blocks of Figure 5b for which internal correlations $C_{ij} > 0.45$ are found. Purple: regions for which $F_{ij} < 0.5$ Å and $C_{ij} > 0.45$. Off diagonal correlations not shown.

at least moderately-correlated displacements. This map is sparse. However, some small groups of atoms obeying the criteria can be found. These include the first strand in the α domain and the N-terminal section of helix A (residues 1−7), residues 42−47 corresponding to strand 2, and residues 50−60 which consist of strands 3 and 4 with the loop between them. Off-diagonal groups of atoms satisfying the criteria include residues 73−80 (a part of the loop between strand 4 and 3_{10} helix in the β-domain) that forms a rigid-body with and is correlated with residues 62−64 (another part of the same loop). On Figure 7 are drawn the regions of low relative fluctuation, regions of moderate average correlation, and regions of both.

CONCLUSIONS

Not all atomic motions in proteins will have functional importance.[32] However, the availability of different conformational states is critical to function in many proteins,[11,12,33] and it is the characterization of these states that is of primary interest here.

The main conclusion of the present article concerns the comparison between nonlocal interatomic distance *fluctuations* and *correlations*. It is demonstrated that those parts of the protein that undergo low interatomic distance fluctuations do not necessarily exhibit the most correlated motion. The fluctuation matrix gives information on the degree of rigidity of the group of atoms considered, whereas the correlation matrix describes the degree of concertation of the atomic motions. Consequently, the distance between two atoms can vary only slightly, leading to a low value of F_{ij} and their belonging to a rigid body, but the fluctuations of one of the atoms can, in principle, be independent of those of the other at all times ($C_{ij} = 0$) or totally correlated ($C_{ij} = 1$). Inversely, the distance between two atoms can be subject to large variation (non-rigid-body behavior, high F_{ij}) and can be either correlated or noncorrelated.

However, some common features to the fluctuation and correlation maps have been pointed out. Low fluctuations and high correlations both are persistent for ∼3 residues along the sequence. Moreover, it has been shown that the secondary structure elements which exhibit a high degree of rigidity combined with moderate correlations are predominantly β strands, whereas only parts of helices are found to be rigid or correlated.

Finally, we note that the correlation maps have not converged over the 1 ns time scale of the simulation, *i.e.*, the calculated maps for the four molecules are markedly different. This is a common problem in the calculation of collective variable properties from MD simulations and indicates the existence of motions in the system on time scales equivalent or longer than the simulation length. It is consistent with previous results on the convergence properties of diffuse scattering intensities.[30,31]

REFERENCES AND NOTES

(1) Cusack, S.; Smith, J. C.; Finney, J. L.; Tidor, B.; Karplus, M. Inelastic Neutron Scattering Analysis of Picosecond Internal Protein Dynamics: Comparison of Harmonic Theory with Experiment. *J. Mol. Biol.* **1988**, *202*, 903−908.
(2) Smith, J. C.; Cusack, S.; Tidor, B.; Karplus, M. Inelastic Neutron Scattering Analysis of Low-Frequency Motions in Proteins: Harmonic and Damped Harmonic Models of BPTI. *J. Chem. Phys.* **1990**, *93*(*5*), 2974−2991.
(3) Hayward, S.; Kitao, A.; Hirata, F.; Go, N. Effect of Solvent on Collective Motions in Globular Protein. *J. Mol. Biol.* **1993**, *234*, 1207−1217.
(4) Becker, O. M.; Karplus, M. Temperature Echoes in Molecular Dynamics Simulations of Proteins. *Phys. Rev. Lett.* **1993**, *70*(*22*), 3514−3517.
(5) Yoshioki, S. Internal Dynamics of a Globular Protein under External Force Field. *J. Comput. Chem.* **1994**, *15*(*7*), 684−703.
(6) Furois-Corbin, S.; Smith, J. C.; Kneller, G. R. Picosecond Timescale Rigid-Helix and Side-Chain Motions in Deoxymyoglobin. *Proteins: Struct. Funct. Genetics.* **1993**, *16*(*2*), 141−154.
(7) Vos, M. H.; Rappaport, F.; Lambry, J.-C.; Breton, J.; Martin, J.-L. Visualization of Coherent Nuclear Motion in a Membrane Protein by Femtosecond Spectroscopy. *Nature* **1993**, *363*, 320−325.
(8) Smith J. C. Protein Dynamics: Comparison of Simulations with Inelastic Neutron Scattering Experiments. *Q. Rev. Biophys.* **1991**, *24*(*3*), 227−291.
(9) Doster, W.; Cusack, S.; Petry, W. Dynamical Transition in Myoglobin Revealed by Inelastic neutron Scattering. *Nature* **1989**, *337*, 754−756.
(10) Smith, J. C.; Kuczera, K.; Karplus, M. Temperature-Dependence of Myoglobin Dynamics: Neutron Spectra Calculated from Molecular Dynamics Simulations of Myoglobin. *Proc. Natl. Acad. Sci. U.S.A.* **1990**, *87*, 1601−1605.
(11) Rasmussen, B. F.; Stock, A. M.; Ringe, D.; Petsko, G. A. Crystalline Ribonuclease A loses Function Below the Dynamical Transition at 220 K. *Nature* **1992**, *357*, 423−424.
(12) Ferrand, M.; Dianoux, A. J.; Petry, W.; Zaccai, G. Thermal Motions and Function of Bacteriorhodopsin in Purple Membranes: Effects of Temperature and Hydratation Studied by Neutron Scattering. *Proc. Natl. Acad. Sci. U.S.A.* **1993**, *90*, 9668−9672.
(13) Elber, R.; Karplus, M. Multiple Conformational States of Proteins: A Molecular Dynamics Analysis of Myoglobin. *Science* **1987**, *235*, 318−321.
(14) Smith, J. C.; Kneller, G. R. Combination of Neutron Scattering and Molecular Dynamics for the Determination of Internal Motions in Biomolecules. *Mol. Simul.* **1993**, *10*, 363−375.
(15) Kneller, G. R.; Smith, J. C. Liquid-like Side-chain Dynamics in Myoglobin. J. *Mol. Biol.* **1994**, *242*, 181−185.
(16) Furois-Corbin, S.; Smith, J. C.; Lavery, R. Low-frequency Vibrations in α-helices: Helicoïdal Analysis of Polyalanine and Deoxymyoglobin Molecular Dynamics Trajectories. *Biopolymers* **1995**, *35*, 555−571.
(17) Caspar, D. L. D.; Clarage, J.; Salunke, D. M.; Clarage, M. Liquid-like Movements in Crystalline Insulin. *Nature* **1988**, *332*, 659−662.
(18) Clarage, J.; Clarage, M.; Phillips, W.; Sweet, R.; Caspar, D. Correlations of Atomic Movements in Lysozyme Crystals. *Proteins: Struct. Funct. Genetics* **1992**, *12*, 145−157.
(19) Gerstein, M.; Lesk, A. M.; Chothia, C. Structural Mechanisms for Domain Movements in Proteins. *Biochemistry* **1994**, *33*(*22*), 6739−6749.
(20) Faure, P.; Micu, A.; Doucet, J.; Smith, J. C.; Benoît, J.-P. Correlated Intramolecular Motions and Diffuse X-Ray Scattering in Lysozyme. *Nature Struct. Biol.* **1994**, *2*, 124−128.
(21) Berthou, J.; Litchitz, A.; Artymiuk, P.; Jollès, P. An X-Ray Study of the Physiological-Temperature Form of Hen Egg-White Lysozyme at 2 Å Resolution. *Proc. R. Soc. Lond.* **1983**, *B217*, 471−489.
(22) Jorgensen, W. L.; Chandrasekhar, J.; Madura, J. D. Comparison of Simple Potential Functions for Simulating Liquid Water. *J. Chem. Phys.* **1983**, *79*, 926−935.
(23) Jollès, P.; Berthou, J. High Temperature Crystallization of Lysozyme: An Example of Phase Transition. *Febs. Lett.* **1972**, *23*, 21−23.
(24) Brooks, B. R.; Bruccoleri, R. E.; Olafson, B. D.; States, D. J.; Swaminathan, S.; Karplus, M. CHARMM: A Programm for Macro-

molecular Energy, Minimization and Dynamics Calculations. J. *Comput. Chem.* **1983**, *4*, 187−217.
(25) Ryckaert, J. P.; Ciccotti, G.; Berendsen, H. J. Numerical Integration of the Cartesian Equations of Motion of a System with Constrains: Molecular Dynamics of N-alkanes. *J. Comp. Phys.* **1977**, *107*, 327−341.
(26) Ichiye, T.; Karplus, M. Collective Motions in Proteins: A Covariance Analysis of Atomic Fluctuations in Molecular Dynamics and Normal Mode Simulations. *Proteins* **1991**, *11*, 205−217.
(27) Briki, F.; Genest, D. Canonical Analysis of Correlated Atomic Motions in DNA from Molecular Dynamics Simulation. *Biophys. Chem.* **1994**, *52*, 35−43.
(28) Saporta, G. In *Probabilites, Analyses de données Statistiques.* Technip: Paris, 1990; Chapter 9, p 187.
(29) Briki, F.; Genest, D. Rigid-Body Motions of Sub-Units in DNA: A Correlation Analysis of a 200 ps Molecular Dynamics Simulation. *J. Biomol. Struct. Dyn.* **1995**, *12*(5), 1063−1082.
(30) Héry, S. Molecular dynamics simulation of crystalline HEW lysozyme: analysis of X-ray diffuse scattering patterns. DEA Thesis, 1994.
(31) Clarage, J. B.; Romo, T.; Andrews, B. K.; Pettitt, B. M.; Phillips, G. N. A Sampling Problem in Molecular Dynamics Simulations of Macromolecules. *Proc. Natl. Acad. Sci. U.S.A.* **1995**, *92*, 3288−3292.
(32) Warshel, A.; Sussman, F.; Hwang, J. K. Evaluation of catalytic Free Energies in Genetically Modified proteins. *J. Mol. Biol.* **1988**, *201*, 139−159.
(33) Huber, R.; Bennett, W. S. Functional Significance of Flexibility in Proteins. *Biopolymers* **1983**, *22*, 261−279.

CI970234A